Shape universality classes in the random sequential addition of non-spherical particles

Baule, A

Shape universality classes in the random sequential addition of non-spherical particles

Adrian Baule[1]
[1] *School of Mathematical Sciences, Queen Mary University of London, Mile End Road, London E1 4NS, UK* *

Random sequential addition (RSA) models are used in a large variety of contexts to model particle aggregation and jamming. A key feature of these models is the algebraic time dependence of the asymptotic jamming coverage as $t \to \infty$. For the RSA of monodisperse non-spherical particles the scaling is generally believed to be $t^{-\nu}$, where $\nu = 1/d_{\rm f}$ for a particle with $d_{\rm f}$ degrees of freedom. While the $d_{\rm f} = 1$ result of spheres (Renyi's classical car parking problem) can be derived analytically, evidence for the $1/d_{\rm f}$ scaling for arbitrary particle shapes has so far only been provided from empirical studies on a case-by-case basis. Here, we show that the RSA of arbitrary non-spherical particles, whose centres of mass are constrained to fall on a line, can be solved analytically for moderate aspect ratios. The asymptotic jamming coverage is determined by a Laplace-type integral, whose asymptotics is fully specified by the contact distance between two particles of given orientations. The analysis of the contact function r shows that the scaling exponent depends on particle shape and falls into two universality classes for generic shapes with $\tilde{d}$ orientational degrees of freedom: (i) $\nu = 1/(1 + \tilde{d}/2)$ when r is a smooth function of the orientations as for smooth convex shapes, e.g., ellipsoids; (ii) $\nu = 1/(1+\tilde{d})$ when r contains singularities due to flat sides as for, e.g., spherocylinders and polyhedra. The exact solution explains in particular why many empirically observed scalings in $2d$ and $3d$ fall in between these two limiting values.

arXiv:1611.03034v1 [cond-mat.stat-mech] 9 Nov 2016

The question of how particle shape affects the dynamical and structural properties of particle aggregates is one of the outstanding problems in statistical mechanics with profound technological implications [1, 2]. Recently, it has become clear that also in the athermal regime the variation of particle shape allows the design of jammed granular materials with specific optimized properties [3]. However, a systematic exploration of the effect of shape variation in jammed systems relies on extensive computer simulations [4–7] or mean-field theories whose solutions require similar computational efforts [8, 9]. From a theoretical perspective, it is striking that so far there has been hardly any insight into the effect of shape variation from exactly solvable analytical models, even though these are most suitable to identify and classify shapes in the infinite shape space. In this letter, we consider the probably simplest non-trivial packing model that takes into account excluded volume effects due to asphericities, namely the random sequential addition (RSA) of particles. The essential packing mechanism in RSA is to select the particles' positions and orientations with uniform probability and then place them sequentially into a given domain if there is no overlap with any previously placed particles. Particles are not able to move or reorient once being placed. Since Renyi's seminal work on the 'car parking problem' (the RSA of monodisperse spheres on a line) [10, 11], RSA models have been widely used to model particle aggregation and jamming in physical, chemical and biological systems [12, 13]. Two key features of these models are: (i) the existence of a finite jamming density ϕ in the infinite time limit $\phi(\infty) = \lim_{t\to\infty} \phi(t)$ and (ii) the algebraic time dependence of the approach to jamming, which is generally assumed to take the form $\phi(\infty) - \phi(t) \sim t^{-\nu}$, where $\nu = 1/d_{\rm f}$ and $d_{\rm f}$ is the number of degrees of freedom of a single particle including d translational and $d_{\rm f}$ orientational ones: $d_{\rm f} = d + \tilde{d}$. Both empirical and theoretical arguments for the validity of $\nu = 1/d_{\rm f}$ have been given. It has been first rationalized for the RSA of spheres in d dimensions [14, 15] confirming early simulation results [16]. For non-spherical particles of finite width [36], $\nu = 1/d_{\rm f}$ has been shown to hold in simulations of ellipses [17–19], rectangles [19–22], and spherocylinders [19]. Approximate theoretical arguments based on the geometry of target sites in the later stages of the RSA process have also been presented [17, 19, 23].

We consider the RSA of non-spherical particles of arbitrary dimensions whose centres of mass are constrained to fall on a $1d$ line (also called the 'Paris car parking problem' in the case of $2d$ particles [24]). Let $p(x, t; \boldsymbol{\alpha}, \boldsymbol{\beta})$ denote the probability to find a segment of length x at time t with a particle of orientation $\boldsymbol{\alpha}$ at the left boundary of the x interval and of orientation $\boldsymbol{\beta}$ at the right one. The vector $\boldsymbol{\alpha} = (\alpha_1, \alpha_2, ..., \alpha_{\tilde{d}})$ contains the angles describing the particle's $\tilde{d}$ orientational degrees of freedom. The master equation for the time evolution of p in dimensionless form is given as

$$\frac{\partial}{\partial t} p(x,t;\boldsymbol{\alpha},\boldsymbol{\beta}) = -\psi(x,\boldsymbol{\alpha},\boldsymbol{\beta}) p(x,t;\boldsymbol{\alpha},\boldsymbol{\beta}) + \left\langle \int_{x+r(\boldsymbol{\beta},\boldsymbol{\gamma})}^{\infty} {\rm d}y\, p(y,t;\boldsymbol{\alpha},\boldsymbol{\gamma}) \right\rangle_{\boldsymbol{\gamma}} + \left\langle \int_{x+r(\boldsymbol{\gamma},\boldsymbol{\alpha})}^{\infty} {\rm d}y\, p(y,t;\boldsymbol{\gamma},\boldsymbol{\beta}) \right\rangle_{\boldsymbol{\gamma}}. \quad (1)$$

Here, the brackets denote an expected value with respect to the isotropic distribution of the orientational angles: $\langle h(\boldsymbol{\gamma})\rangle_{\boldsymbol{\gamma}} = C^{-1}\int \mathrm{d}\boldsymbol{\gamma}\, h(\boldsymbol{\gamma})$, where C is a normalization constant. The function ψ is defined as

$$\psi(x,\boldsymbol{\alpha},\boldsymbol{\beta}) = \left\langle (x - r(\boldsymbol{\alpha},\boldsymbol{\gamma}) - r(\boldsymbol{\gamma},\boldsymbol{\beta}))^{+}\right\rangle_{\boldsymbol{\gamma}}. \tag{2}$$

where $(x)^+ = x$ for $x > 0$ and $(x)^+ = 0$ for $x \leq 0$. The central quantity capturing the effect of anisotropic shapes is $r(\boldsymbol{\alpha},\boldsymbol{\beta})$ denoting the contact distance of two shapes of orientations $\boldsymbol{\alpha}$ and $\boldsymbol{\beta}$. Here, the contact point of the two particles can lie away from the axis depending on the particles' orientations. In Eq. (1), the first term on the rhs denotes the probability that an interval $x,\boldsymbol{\alpha},\boldsymbol{\beta}$ is destroyed by placing a particle inside it (ψ describes the number of ways this can be done). Likewise, the two integrals in Eq. (1) describe the creation of an interval $x,\boldsymbol{\alpha},\boldsymbol{\beta}$ by placing a particle into a larger interval. Eq. (1) recovers as special cases several models discussed previously in the literature. It trivially recovers the exactly solvable monodisperse sphere case [10, 11, 25, 26]. The next simplest model is the RSA of polydisperse spheres with a uniform size distribution [27–29], which can be mapped onto Eq. (1). Even for this simple extension the aymptotic scaling has not been obtained so far. The special case of bidisperse spheres has been treated in [30] showing an algebraic decay $\nu = 1$ due to the small spheres, while the contribution of the large spheres decays exponentially. The two dimensional version of Eq. (1) has been studied within an approximate analytical approach in [31] for the case of rectangles with long aspect ratios, where the scaling $\nu = 1/d_\mathrm{f} = 1/2$ could be confirmed. The related problem of two dimensional non-spherical particles on a line at thermal equilibrium has been discussed in [32, 33].

Eq. (1) separates into three different regimes depending on x

$$p(x,t;\boldsymbol{\alpha},\boldsymbol{\beta}) = \begin{cases} p_1(x,t;\boldsymbol{\alpha},\boldsymbol{\beta}), & x > g_2(\boldsymbol{\alpha},\boldsymbol{\beta}) \\ p_2(x,t;\boldsymbol{\alpha},\boldsymbol{\beta}), & g_1(\boldsymbol{\alpha},\boldsymbol{\beta}) \leq x \leq g_2(\boldsymbol{\alpha},\boldsymbol{\beta}) \\ p_3(x,t;\boldsymbol{\alpha},\boldsymbol{\beta}), & r(\boldsymbol{\alpha},\boldsymbol{\beta}) \leq x < g_1(\boldsymbol{\alpha},\boldsymbol{\beta}) \end{cases} \tag{3}$$

Regime 1 corresponds to the case when x is large enough such that a particle can be inserted between the two boundary particles with an arbitrary orientation. Orientations are restricted in regime 2 up to $x = g_1(\boldsymbol{\alpha},\boldsymbol{\beta})$, below which no particle can be inserted anymore. In regime 3 intervals can thus only be created but not destroyed. The three regimes are thus distinguished by the two functions

$$g_1(\boldsymbol{\alpha},\boldsymbol{\beta}) = \min_{\boldsymbol{\gamma}}\left[r(\boldsymbol{\alpha},\boldsymbol{\gamma}) + r(\boldsymbol{\gamma},\boldsymbol{\beta})\right] \tag{4}$$

$$g_2(\boldsymbol{\alpha},\boldsymbol{\beta}) = \max_{\boldsymbol{\gamma}}\left[r(\boldsymbol{\alpha},\boldsymbol{\gamma}) + r(\boldsymbol{\gamma},\boldsymbol{\beta})\right]. \tag{5}$$

Defining the upper and lower limits of r as $a \leq r(\boldsymbol{\alpha},\boldsymbol{\beta}) \leq b$, we see that $2a \leq g_1(\boldsymbol{\alpha},\boldsymbol{\beta}) \leq g_2(\boldsymbol{\alpha},\boldsymbol{\beta}) \leq 2b$. The quantity of main interest in the RSA process is the number density of particles (the 1d equivalent of packing density) as a function of time, which can be obtained as

$$\phi(t) = \int \mathrm{d}\boldsymbol{\alpha} \int \mathrm{d}\boldsymbol{\beta} \int_{r(\boldsymbol{\alpha},\boldsymbol{\beta})}^{\infty} \mathrm{d}x\, p(x,t;\boldsymbol{\alpha},\boldsymbol{\beta}). \tag{6}$$

It turns out that for particles with small aspect ratios, the equations describing the three different regimes decouple in a way that analytical expressions for $p_{1,2,3}$ can be obtained. We first note that in regime 1, we have with Eq. (2):

$$\psi(x,\boldsymbol{\alpha},\boldsymbol{\beta}) = x - \langle r(\boldsymbol{\alpha},\boldsymbol{\gamma})\rangle_{\boldsymbol{\gamma}} - \langle r(\boldsymbol{\gamma},\boldsymbol{\beta})\rangle_{\boldsymbol{\gamma}}. \tag{7}$$

In order to solve the master equation for p_1 we can thus make a similar ansatz as in Renyi's car parking problem, which is solved by $p(x,t) = t^2F(t)e^{-xt}$, where $F(t)$ satisfies the ODE $\dot{F}(t) = 2F(t)\left(1-\left(1-e^{-t}\right)/t\right)$, assuming a unit diameter of the spheres and the initial condition is $F(0) = 1$. For Eq. (1) with ψ given as in Eq. (7) we make the ansatz

$$p_1(x,t;\boldsymbol{\alpha},\boldsymbol{\beta}) = t^2F(t,\boldsymbol{\alpha},\boldsymbol{\beta})e^{-xt} \tag{8}$$

Substituting into Eq. (1) yields

$$\begin{aligned}\frac{\partial}{\partial t}F(t,\boldsymbol{\alpha},\boldsymbol{\beta}) &= (\langle r(\boldsymbol{\alpha},\boldsymbol{\gamma})\rangle_{\boldsymbol{\gamma}} + \langle r(\boldsymbol{\gamma},\boldsymbol{\beta})\rangle_{\boldsymbol{\gamma}})F(t,\boldsymbol{\alpha},\boldsymbol{\beta}) \\ &\quad -\frac{2F(t,\boldsymbol{\alpha},\boldsymbol{\beta})}{t} + \frac{1}{t}\left\langle F(t,\boldsymbol{\alpha},\boldsymbol{\gamma})e^{-r(\boldsymbol{\beta},\boldsymbol{\gamma})t}\right\rangle_{\boldsymbol{\gamma}} \\ &\quad +\frac{1}{t}\left\langle F(t,\boldsymbol{\gamma},\boldsymbol{\beta})e^{-r(\boldsymbol{\gamma},\boldsymbol{\alpha})t}\right\rangle_{\boldsymbol{\gamma}}.\end{aligned} \tag{9}$$

The key observation is that also the master equation for p_2 can be solved analytically when

$$g_1(\boldsymbol{\alpha},\boldsymbol{\beta}) + a \geq g_2(\boldsymbol{\alpha},\boldsymbol{\beta}). \tag{10}$$

In this case, the integral terms in Eq. (1) only integrate over p_1, which is given by Eq. (8). The geometric reason is that in this case one can maximally insert a single particle in any x-interval in regime 2. As a consequence, p_2 satisfies a simple first-order ODE with an inhomogeneity given by the integral terms. The solution is obtained directly and can be expressed in the form

$$\begin{aligned}p_2(x,t;\boldsymbol{\alpha},\boldsymbol{\beta}) &= p_1(x,t;\boldsymbol{\alpha},\boldsymbol{\beta}) + \Big[x - \langle r(\boldsymbol{\alpha},\boldsymbol{\gamma})\rangle_{\boldsymbol{\gamma}} \\ &\quad - \langle r(\boldsymbol{\gamma},\boldsymbol{\beta})\rangle_{\boldsymbol{\gamma}} - \psi(x,\boldsymbol{\alpha},\boldsymbol{\beta})\Big] \\ &\quad \times \int_0^t \mathrm{d}s e^{-\psi(x,\boldsymbol{\alpha},\boldsymbol{\beta})(t-s)}p_1(x,s;\boldsymbol{\alpha},\boldsymbol{\beta}).\end{aligned} \tag{11}$$

Ensuring that Eq. (10) holds for all angles $\boldsymbol{\alpha},\boldsymbol{\beta}$ requires that $3a \geq 2b$. For regular convex particles, a, b can be identified with the width and length of the particles, respectively. In this case, Eq. (10) is equivalent to considering particles with an aspect ratio ≤ 1.5. Since the integral terms in the master equation for p_3 only contain $p_{1,2}$, we can likewise express p_3 analytically with the solutions Eqs. (8,11), such that p is fully specified with the solution $F(t, \boldsymbol{\alpha}, \boldsymbol{\beta})$ of Eq. (9).

Unfortunately, since the contact distance is in general a highly complicated function, which already in the case of ellipsoids can not be expressed in closed form [34], solving Eq. (9) analytically is not feasible in general. However, the asymptotic jamming coverage can still be investigated analytically. In order to obtain $\phi(\infty) - \phi(t)$ we need to calculate

$$\begin{aligned}&\phi(\infty) - \phi(t)\\&= \int \mathrm{d}\boldsymbol{\alpha} \int \mathrm{d}\boldsymbol{\beta} \int_{r(\boldsymbol{\alpha},\boldsymbol{\beta})}^{\infty} \mathrm{d}x \int_t^{\infty} \mathrm{d}s \frac{\partial p}{\partial s}(x, s; \boldsymbol{\alpha}, \boldsymbol{\beta}). \quad (12)\end{aligned}$$

Substituting the master equation for the time derivative, we see that we need to evaluate time integrals of $p_{1,2}$. The key to express these analytically for large t is the observation that $F(t, \boldsymbol{\alpha}, \boldsymbol{\beta})$ scales in this regime as (see Eq. (9))

$$\begin{aligned}F(t, \boldsymbol{\alpha}, \boldsymbol{\beta}) &\approx e^{\left(\langle r(\boldsymbol{\alpha},\boldsymbol{\gamma})\rangle_{\boldsymbol{\gamma}} + \langle r(\boldsymbol{\gamma},\boldsymbol{\beta})\rangle_{\boldsymbol{\gamma}}\right)(t-t_c) - 2\int_{t_c}^{t} \mathrm{d}s\, \frac{1}{s}}\\&\sim t^{-2} e^{\left(\langle r(\boldsymbol{\alpha},\boldsymbol{\gamma})\rangle_{\boldsymbol{\gamma}} + \langle r(\boldsymbol{\gamma},\boldsymbol{\beta})\rangle_{\boldsymbol{\gamma}}\right)t}, \quad (13)\end{aligned}$$

where t_c is a lower cutoff whose contribution can be neglected as $t \to \infty$. Therefore, we have $p_1(x, t; \boldsymbol{\alpha}, \boldsymbol{\beta}) \sim e^{-(x - \langle r(\boldsymbol{\alpha},\boldsymbol{\gamma})\rangle_{\boldsymbol{\gamma}} - \langle r(\boldsymbol{\gamma},\boldsymbol{\beta})\rangle_{\boldsymbol{\gamma}})t}$ and

$$\int_t^{\infty} \mathrm{d}s\, p_1(x, s; \boldsymbol{\alpha}, \boldsymbol{\beta}) \sim \frac{e^{-(x - \langle r(\boldsymbol{\alpha},\boldsymbol{\gamma})\rangle_{\boldsymbol{\gamma}} - \langle r(\boldsymbol{\gamma},\boldsymbol{\beta})\rangle_{\boldsymbol{\gamma}})t}}{x - \langle r(\boldsymbol{\alpha},\boldsymbol{\gamma})\rangle_{\boldsymbol{\gamma}} - \langle r(\boldsymbol{\gamma},\boldsymbol{\beta})\rangle_{\boldsymbol{\gamma}}} \quad (14)$$

The scaling of the convolution integral in Eq. (11) can thus be evaluated as well and leads to

$$\int_t^{\infty} \mathrm{d}s\, p_2(x, s; \boldsymbol{\alpha}, \boldsymbol{\beta}) \sim \frac{1}{\psi(x, \boldsymbol{\alpha}, \boldsymbol{\beta})} e^{-\psi(x,\boldsymbol{\alpha},\boldsymbol{\beta})t}. \quad (15)$$

From Eq. (12) we obtain with some manipulations and using Eqs. (14,15)

$$\begin{aligned}&\phi(\infty) - \phi(t) \sim\\&\int \mathrm{d}\boldsymbol{\alpha} \int \mathrm{d}\boldsymbol{\beta} \int_{g_2(\boldsymbol{\alpha},\boldsymbol{\beta})}^{\infty} \mathrm{d}x\, e^{-(x - \langle r(\boldsymbol{\alpha},\boldsymbol{\gamma})\rangle_{\boldsymbol{\gamma}} - \langle r(\boldsymbol{\gamma},\boldsymbol{\beta})\rangle_{\boldsymbol{\gamma}})t}\\&+ \int \mathrm{d}\boldsymbol{\alpha} \int \mathrm{d}\boldsymbol{\beta} \int_{g_1(\boldsymbol{\alpha},\boldsymbol{\beta})}^{g_2(\boldsymbol{\alpha},\boldsymbol{\beta})} \mathrm{d}x\, e^{-\psi(x,\boldsymbol{\alpha},\boldsymbol{\beta})t} \quad (16)\end{aligned}$$

Since $\langle r(\boldsymbol{\alpha},\boldsymbol{\gamma})\rangle_{\boldsymbol{\gamma}} + \langle r(\boldsymbol{\gamma},\boldsymbol{\beta})\rangle_{\boldsymbol{\gamma}} > g_2(\boldsymbol{\alpha},\boldsymbol{\beta})$, the first term decays exponentially for $t \to \infty$. The asymptotic scaling is thus determined by evaluating the asymptotics of the second Laplace-type integral. To this end we need to investigate the stationary points of ψ. The definitions of ψ and g_1 imply that $\psi(g_1(\boldsymbol{\alpha},\boldsymbol{\beta}), \boldsymbol{\alpha}, \boldsymbol{\beta}) = 0$ and $\nabla\psi(g_1(\boldsymbol{\alpha},\boldsymbol{\beta}), \boldsymbol{\alpha}, \boldsymbol{\beta}) = 0$, so the stationary points lie on the surface $x = g_1(\boldsymbol{\alpha},\boldsymbol{\beta})$ on the boundary of the integration region and correspond to minima since $\psi \geq 0$. The asymptotics of such a high-dimensional Laplace integral with degenerate stationary points is typically highly challenging. The analysis in the present case is possible since the behaviour of ψ for x close to the minima can be determined analytically, which determines the properties of the integral for large t. Using Eq. (2) we can write

$$\psi(x, \boldsymbol{\alpha}, \boldsymbol{\beta}) = \frac{1}{C} \sum_{i=1}^{n} \int_{\Omega_i} \mathrm{d}\boldsymbol{\gamma} (x - r(\boldsymbol{\alpha},\boldsymbol{\gamma}) - r(\boldsymbol{\gamma},\boldsymbol{\beta})), \quad (17)$$

where it is assumed that there are n $\tilde{d}$-dimensional domains $\Omega_i(x, \boldsymbol{\alpha}, \boldsymbol{\beta})$ where $\psi \geq 0$, i.e., Ω_i is bounded by hypersurfaces satisfying

$$x = r(\boldsymbol{\alpha},\boldsymbol{\gamma}) + r(\boldsymbol{\gamma},\boldsymbol{\beta}). \quad (18)$$

We assume that there exists a unique global minimum $\boldsymbol{\gamma}^*(\boldsymbol{\alpha},\boldsymbol{\beta})$ for any $\boldsymbol{\alpha},\boldsymbol{\beta}$ corresponding to the $\boldsymbol{\gamma}$ value defining $g_1(\boldsymbol{\alpha},\boldsymbol{\beta})$ in Eq. (4). The existence of a unique minimum is not a priori clear, but can be expected for generic shapes (see the discussion below). As $x \to g_1(\boldsymbol{\alpha},\boldsymbol{\beta})$ only the interval i_{m} containing $\boldsymbol{\gamma}^*$ remains in the sum in Eq. (17). Expanding around $\boldsymbol{\gamma}^*$ thus yields to leading order

$$\psi(x, \boldsymbol{\alpha}, \boldsymbol{\beta}) \approx \frac{1}{C}(x - g_1(\boldsymbol{\alpha},\boldsymbol{\beta}))\Omega_{i_{\mathrm{m}}}(x, \boldsymbol{\alpha}, \boldsymbol{\beta}). \quad (19)$$

The volume $\Omega_{i_{\mathrm{m}}}$ is centred at $\boldsymbol{\gamma}^*$ and constrained to become smaller and smaller for $x \to g_1(\boldsymbol{\alpha},\boldsymbol{\beta})$. If we introduce the vector $\boldsymbol{\epsilon} = \boldsymbol{\gamma} - \boldsymbol{\gamma}^*$ and switch to spherical coordinates $\boldsymbol{\epsilon} = z(\boldsymbol{\theta})\hat{\mathbf{u}}(\boldsymbol{\theta})$, where $\boldsymbol{\theta}$ parametrizes the solid angle in $\tilde{d}$ dimensions and $\hat{\mathbf{u}}$ is a unit vector, we can calculate $\Omega_{i_{\mathrm{m}}}$ as

$$\Omega_{i_{\mathrm{m}}} = \oint \mathrm{d}\boldsymbol{\theta} \int_0^{z(\boldsymbol{\theta})} \mathrm{d}z\, z^{\tilde{d}-1} = \oint \mathrm{d}\boldsymbol{\theta}\, z(\boldsymbol{\theta})^{\tilde{d}}, \quad (20)$$

where $z(\boldsymbol{\theta})$ denotes the boundary of the volume $\Omega_{i_{\mathrm{m}}}$ in the direction of a given solid angle $\boldsymbol{\theta}$ and $\mathrm{d}\boldsymbol{\theta}$ includes the surface element in $\tilde{d}$ dimensions. This means that $z(\boldsymbol{\theta}) = z(\boldsymbol{\theta}; x, \boldsymbol{\alpha}, \boldsymbol{\beta})$ and is determined by the condition Eq. (18). In order to determine z, we develop Eq. (18) around $\boldsymbol{\gamma}^*$. This yields up to quadratic orders

$$x \approx g_1(\boldsymbol{\alpha},\boldsymbol{\beta}) + \mathbf{h}\,\boldsymbol{\epsilon} + \boldsymbol{\epsilon}^{\mathrm{T}}\mathrm{M}\boldsymbol{\epsilon}, \quad (21)$$

where

$$\begin{aligned}\mathbf{h}(\boldsymbol{\alpha},\boldsymbol{\beta}) &= \nabla_{\boldsymbol{\gamma}} r(\boldsymbol{\alpha},\boldsymbol{\gamma}^*) + \nabla r_{\boldsymbol{\gamma}}(\boldsymbol{\gamma}^*,\boldsymbol{\beta}) \quad (22)\\\mathrm{M}(\boldsymbol{\alpha},\boldsymbol{\beta}) &= \nabla_{\boldsymbol{\gamma}}\nabla_{\boldsymbol{\gamma}} r(\boldsymbol{\alpha},\boldsymbol{\gamma}^*) + \nabla_{\boldsymbol{\gamma}}\nabla_{\boldsymbol{\gamma}} r(\boldsymbol{\gamma}^*,\boldsymbol{\beta}). \quad (23)\end{aligned}$$

Eq. (21) allows us to establish the functional form of ψ depending on the particle shape. For generic smooth shapes, the contact distance $r(\boldsymbol{\alpha},\boldsymbol{\beta})$ is a smooth function of the two sets of angles. Therefore, $r(\boldsymbol{\alpha},\boldsymbol{\gamma}) + r(\boldsymbol{\gamma},\boldsymbol{\beta})$ is smooth around the minimum at $\boldsymbol{\gamma}^*$ in all directions and we always have $\mathbf{h}(\boldsymbol{\alpha},\boldsymbol{\beta}) = \mathbf{0}$. As a consequence $z(\boldsymbol{\theta};x,\boldsymbol{\alpha},\boldsymbol{\beta})$ is given by $z = \sqrt{x - g_1(\boldsymbol{\alpha},\boldsymbol{\beta})/(\hat{\mathbf{u}}(\boldsymbol{\theta})^{\mathrm{T}}\mathrm{M}(\boldsymbol{\alpha},\boldsymbol{\beta})\hat{\mathbf{u}}(\boldsymbol{\theta}))}$ and the leading order of ψ is with Eqs. (19,20)

$$\psi(x,\boldsymbol{\alpha},\boldsymbol{\beta}) \approx \oint \mathrm{d}\boldsymbol{\theta}\, \frac{(x - g_1(\boldsymbol{\alpha},\boldsymbol{\beta}))^{1+\tilde{d}/2}}{C\left(\hat{\mathbf{u}}(\boldsymbol{\theta})^{\mathrm{T}}\mathrm{M}(\boldsymbol{\alpha},\boldsymbol{\beta})\hat{\mathbf{u}}(\boldsymbol{\theta})\right)^{\tilde{d}}}. \tag{24}$$

For large t, Eq. (16) yields after a variable transformation

$$\phi(\infty) - \phi(t) \sim \int_0^1 \mathrm{d}x\, e^{-x^{1+\tilde{d}/2}t} \sim t^{-1/(1+\tilde{d}/2)} \tag{25}$$

where the upper limit of the x integration is irrelevant since both $g_2(\boldsymbol{\alpha},\boldsymbol{\beta}) - g_1(\boldsymbol{\alpha},\boldsymbol{\beta})$ and $\oint \mathrm{d}\boldsymbol{\theta}\left(\hat{\mathbf{u}}(\boldsymbol{\theta})^{\mathrm{T}}\mathrm{M}(\boldsymbol{\alpha},\boldsymbol{\beta})\hat{\mathbf{u}}(\boldsymbol{\theta})\right)^{-\tilde{d}/(1+\tilde{d}/2)}$ are finite of order one.

On the other hand, if the minimum $\boldsymbol{\gamma}^*$ is singular in some directions, an expansion like Eq. (21) is not possible. In order to elucidate the situation, we consider first the $2d$ case, where r can be approximated in closed analytical form for small angles α,β [32, 33]

$$r(\alpha,\beta) \approx 2a + a_1(\alpha^2 + \beta^2) + a_2|\alpha - \beta|^{\mu}, \tag{26}$$

Here, $a_{1,2}$ are parameters specified by the aspect ratio and μ is a shape dependent parameter $\mu \in [1,2]$. For generic shapes, μ is given by either 1 or 2 depending on whether the contact point is away from the axis or close to it, respectively. For, e.g., ellipses $\mu = 2$ and r is smooth throughout such that the $t^{-2/3}$ scaling holds from Eq. (25) with $\tilde{d} = 1$. For, e.g., rectangles $\mu = 1$ and r is singular when the minimum is at $\gamma^* = \alpha$ or $\gamma^* = \beta$. As a consequence, the deviation from γ^* scales linearly $\epsilon \sim (x - g_1(\alpha,\beta)$ and $\psi(x,\alpha,\beta) \sim (x - g_1(\alpha,\beta))^2$, leading to the asymptotic scaling $t^{-1/2}$ in this case. For non-generic shapes, μ could in principle assume values in the whole range $[1,2]$. The same analysis then predicts $\epsilon \sim (x - g_1(\alpha,\beta)^{1/\mu}$ and $\psi(x,\alpha,\beta) \sim (x - g_1(\alpha,\beta))^{1+1/\mu}$ leading to the scaling $t^{-1/(1+1/\mu)}$. However, since already in $2d$ exact representations of such shapes are not known, it is not clear if the general μ case can be realized at all.

Coming back to the discussion of a general r in arbitrary dimensions for a singular $\boldsymbol{\gamma}^*$, we can infer from Eq. (26) that the behaviour around $\boldsymbol{\gamma}^*$ is likewise governed by an absolute value in one or multiple directions for shapes with flat sides. The integration region $\Omega_{i_{\mathrm{m}}}$ can then be separated in a piecewise way and Eq. (18) close to $\boldsymbol{\gamma}^*$ applied in each of the regions. Since the first order term $\mathbf{h}^{(j)}$ of the jth region does not vanish, we have thus $z^{(j)} = (x - g_1(\boldsymbol{\alpha},\boldsymbol{\beta}))/(\mathbf{h}^{(j)}(\boldsymbol{\alpha},\boldsymbol{\beta})\hat{\mathbf{u}}(\boldsymbol{\theta}))$. The leading term of ψ in this case is

$$\psi(x,\boldsymbol{\alpha},\boldsymbol{\beta}) \approx \sum_{j=1}^{m} \int_j \mathrm{d}\boldsymbol{\theta}\, \frac{(x - g_1(\boldsymbol{\alpha},\boldsymbol{\beta}))^{1+\tilde{d}}}{C\left(\mathbf{h}^{(j)}(\boldsymbol{\alpha},\boldsymbol{\beta})\hat{\mathbf{u}}(\boldsymbol{\theta})\right)^{\tilde{d}}}, \tag{27}$$

assuming m piecewise regions of the integration domain covering different solid angles. The asymptotic scaling is then for arbitrary dimensions

$$\phi(\infty) - \phi(t) \sim \int_0^1 \mathrm{d}x\, e^{-x^{1+\tilde{d}}t} \sim t^{-1/(1+\tilde{d})}. \tag{28}$$

It is important to note that the singular nature of $\boldsymbol{\gamma}^*$ can vary depending on the configurations $\boldsymbol{\alpha},\boldsymbol{\beta}$. Already for rectangles under the approximation Eq. (26), there are many configurations where $\gamma^* \neq \alpha,\beta$ and thus the minimum is smooth. Likewise for spherocylinders in arbitrary dimensions, when the contact point is on the spherical caps. The corresponding regions in $\boldsymbol{\alpha},\boldsymbol{\beta}$ thus need to be separated in the integral Eq. (16), such that the overall scaling is given as a superposition of terms proportional to $t^{-1/(1+\tilde{d}/2)}$ and $t^{-1/(1+\tilde{d})}$. As $t \to \infty$ the $t^{-1/(1+\tilde{d})}$ scaling always dominates, but this might be visible only on very long time scales.

Comparing the theoretical predictions Eqs. (25,28) with simulation data in $2d$, we see that the scaling $t^{-2/3}$ for ellipses ($\tilde{d} = 1$) is indeed observed (see Fig. 1a). The data for rectangles and discorectangles is in between the $t^{-2/3}$ and $t^{-1/2}$ scaling indicating an intermediate time regime, since for these shapes the minimum can be both singular and smooth depending on the configuration α,β. In $3d$, the solution predicts the scaling $\nu = 1/2$ for spheroids ($\tilde{d} = 2$). Again, this scaling is not observed on the time scales accessible in the simulations of Fig. 1a. We can clarify the situation by investigating the minima of the function $r(\boldsymbol{\alpha},\boldsymbol{\gamma}) + r(\boldsymbol{\gamma},\boldsymbol{\beta})$ in $\boldsymbol{\gamma}$, which is plotted in Fig. 1b for a particular configuration $\boldsymbol{\alpha},\boldsymbol{\beta}$. The minima seem continuously degenerate in two directions in the plane spanned by the polar (γ_1) and azimuthal (γ_2) angles: at $\gamma_1 = 0$ due to the rotational symmetry and at $\gamma_2 \approx \pm\pi/2$, where the $\pm$ is due to the up/down symmetry of the shape. Due to the degeneracies there are three regions Ω_i contributing to ψ as $x \to g_1(\boldsymbol{\alpha},\boldsymbol{\beta})$, see Eq. (17). Closer inspection reveals indeed the presence of a global minimum γ^*, which however, is hardly distinguishable. As a consequence, the scaling predicted by the above calculation holds only for long times, where the small differences between the minima dominate the asymptotics of the integral Eq. (16). The pronounced quasi degeneracies are mainly due to the short aspect ratio regime and present for almost all angles $\boldsymbol{\alpha},\boldsymbol{\beta}$. They are reduced for large aspect ratios, where small angular differences can induce more pronounced variations in the contact distance.

In summary, the analytical solution of the generalized 'Paris car parking problem' solves a long standing problem in our understanding of random sequential addition processes highlighting the shape dependence of the scaling exponent. The analysis of the function $r(\boldsymbol{\alpha},\boldsymbol{\gamma})+r(\boldsymbol{\gamma},\boldsymbol{\beta})$ shows the existence of two shape universality classes depending on the presence of singularities at the minimum γ^*, which can be associated with smooth

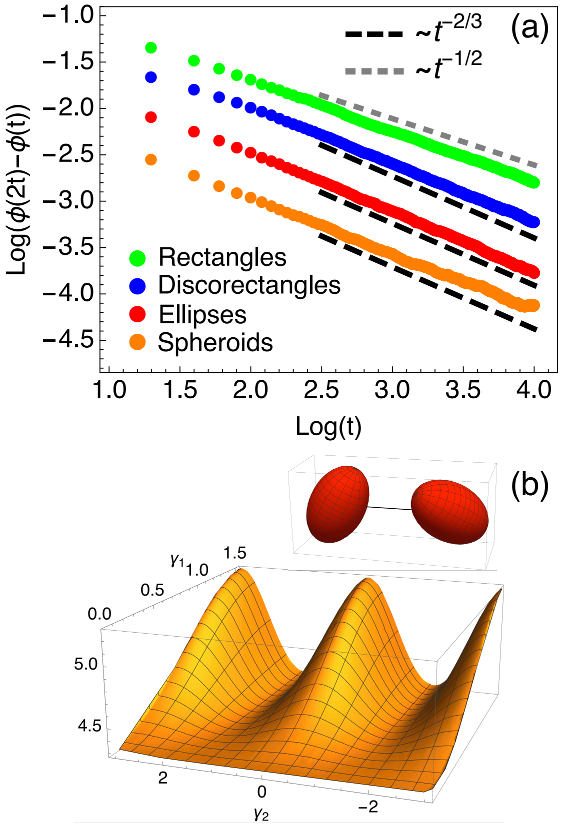

FIG. 1: (Colors online) (a) Plot of simulation results for the asymptotic scaling for a set of shapes with aspect ratio 1.5. Shown is the function $\log(\phi((2t)-\phi(t))$, which exhibits the same scaling as $\log(\phi((\infty)-\phi(t))$ when plotted against $\log(t)$ [20]. For rectangles and discorectangles the empirical exponent falls in the range $1/2 \leq \nu \leq 2/3$ indicating only the intermediate time regime as explained by the theory. (b) A plot of the function $r(\boldsymbol{\alpha},\boldsymbol{\gamma})+r(\boldsymbol{\gamma},\boldsymbol{\beta})$ as a function of $\boldsymbol{\gamma}=(\gamma_1,\gamma_2)$ for spheroids using the algorithm of [34]. The angles $\boldsymbol{\alpha},\boldsymbol{\beta}$ are fixed as in the image. The minima of the function are quasi degenerate at $\gamma_1=0$ and $\gamma_2\approx\pm\pi/2$, such that the predicted $t^{-1/2}$ scaling is only observed for very long times.

convex shapes on the one hand and shapes with flat sides on the other. It is important to note that the Laplace-type integral Eq. (16) is valid for arbitrary shapes, including also non-convex ones. Here, higher order cusp singularities might be present in the contact distance that prevent an expansion like in Eq. (21), leading to non-universal exponents. The solution presented here allows us to fully understand even such exotic cases based on the analytic properties of the contact distance alone.

AB gratefully acknowledges funding under EPSRC grant EP/L020955/1.

* Electronic address: a.baule@qmul.ac.uk

[1] L. Onsager, Ann. N. Y. Acad. Sci. **51**, 627 (1949).
[2] S. Torquato, *Random heterogeneous materials: microstructure and macroscopic properties* (Springer, 2002).
[3] H. M. Jaeger, Soft Matter **11**, 12 (2015).
[4] P. F. Damasceno, M. Engel, and S. C. Glotzer, Science **337**, 453 (2012).
[5] M. Z. Miskin and H. M. Jaeger, Nature Mater. **12**, 326 (2013).
[6] M. Z. Miskin and H. M. Jaeger, Soft Matter **10**, 3708 (2014).
[7] L. K. Roth and H. M. Jaeger, Soft Matter **12**, 1107 (2016).
[8] A. Baule, R. Mari, L. Bo, L. Portal, and H. A. Makse, Nature Commun. **4**, 2194 (2013).
[9] A. Baule and H. A. Makse, Soft Matter **10**, 4423 (2014).
[10] A. Rényi, Publ. Math. Res. Inst. Hung. Acad. Sci. **3**, 109 (1958).
[11] A. Renyi, Sel. Trans. Math. Stat. Prob. **4**, 205 (1963).
[12] J. W. Evans, Rev. Mod. Phys. **65**, 1281 (1993).
[13] J. Talbot, G. Tarjus, P. V. Tassel, and P. Viot, Colloids and Surfaces A **165**, 287 (2000).
[14] Y. Pomeau, J. Phys. A **13**, L193 (1980).
[15] R. H. Swendsen, Phys. Rev. A **24**, 504 (1981).
[16] J. Feder, J. Theor. Biol. **87**, 237 (1980), ISSN 0022-5193.
[17] J. Talbot, G. Tarjus, and P. Schaaf, Phys. Rev. A **40**, 4808 (1989).
[18] J. D. Sherwood, J. Phys. A **23**, 2827 (1990).
[19] P. Viot, G. Tarjus, S. M. Ricci, and J. Talbot, J. Chem. Phys. **97**, 5212 (1992).
[20] R. D. Vigil and R. M. Ziff, J. Chem. Phys. **93**, 8270 (1990).
[21] R. D. Vigil and R. M. Ziff, J. Chem. Phys. **91**, 2599 (1989).
[22] P. Viot and G. Tarjus, EPL **13**, 295 (1990).
[23] G. Tarjus and J. Talbot, J. Phys. A **24**, L913 (1991).
[24] P. M. Chaikin, A. Donev, W. Man, F. H. Stillinger, and S. Torquato, Ind. Eng. Chem. Res. **45**, 6960 (2006).
[25] J. K. Mackenzie, J. Chem. Phys. **37**, 723 (1962).
[26] B. Widom, J. Chem. Phys. **44**, 3888 (1966).
[27] P. E. Ney, Ann. Math. Stat. **33**, 702 (1962).
[28] J. P. Mullooly, J. App. Prob. **5**, 427 (1968).
[29] D. Burridge and Y. Mao, Phys. Rev. E **69**, 037102 (2004).
[30] M. K. Hassan, J. Schmidt, B. Blasius, and J. Kurths, Phys. Rev. E **65**, 045103 (2002).
[31] G. Tarjus and P. Viot, Phys. Rev. Lett. **67**, 1875 (1991).
[32] J. L. Lebowitz, J. K. Percus, and J. Talbot, J. Stat. Phys. **49**, 1221 (1987), ISSN 1572-9613.
[33] Y. Kantor and M. Kardar, EPL **87**, 60002 (2009).
[34] X. Zheng, W. Iglesias, and P. Palffy-Muhoray, Phys. Rev. E **79**, 057702 (2009).
[35] M. D. Khandkar, A. V. Limaye, and S. B. Ogale, Phys. Rev. Lett. **84**, 570 (2000).
[36] Note that the scaling $\nu = 1/d_{\mathrm{f}}$ is violated for infinitely thin particles like needles [20, 31, 35].